Submillisecond-response nematic liquid crystals for augmented reality displays

HAIWEI CHEN, FANGWANG GOU, AND SHIN-TSON WU[*]

College of Optics and Photonics, University of Central Florida, Orlando, FL 32816, USA
[*]swu@ucf.edu

Abstract: We report a new nematic liquid crystal (LC) mixture with an ultra-low rotational viscosity (γ_1 = 53.4 mPas @ 35°C), relatively high birefringence ($\Delta n \approx$0.15), and moderate dielectric anisotropy ($\Delta\varepsilon$ = −2.80 @ 35°C). When employed in a liquid-crystal-on-silicon (LCoS) projector with RGB light-emitting diodes (LEDs), a sub-millisecond response time is obtained without the need for complicated overdrive circuitry. Such a fast response time enables field sequential color display, which not only triples the optical efficiency and resolution density, but also greatly suppresses the image blur and color breakup. Moreover, the required cell gap is 1.2 μm, which is still manageable for high-yield manufacturing. We believe this mixture would find widespread applications for the emerging augmented reality displays.

OCIS codes: (160.3710) Liquid crystals; (230.3720) Liquid-crystal devices; (120.2040) Displays.

References and links

1. D. Armitage, I. Underwood, and S. T. Wu, *Introduction to Miscrodisplay* (John Wiley & Sons, 2006).
2. D. Cuypers, H. De Smet, and A. Van Calster, "VAN LCOS Microdisplays: A decade of technological evolution," J. Disp. Technol. **7**(3), 127–134 (2011).
3. K. Y. Chen, Y. W. Li, K. H. Fan-Chiang, H. C. Kuo, and H. C. Tsai, "Color sequential front-lit LCOS for wearable displays," SID Int. Symp. Digest Tech. Papers **46**(1), 1737–1740 (2015).
4. Z. Luo, F. Peng, H. Chen, M. Hu, J. Li, Z. An, and S. T. Wu, "Fast-response liquid crystals for high image quality wearable displays," Opt. Mater. Express **5**(3), 603–610 (2015).
5. J. Christmas and N. Collings, "Realizing automotive holographic head up displays," SID Int. Symp. Digest Tech. Papers **47**(1), 1017–1020 (2016).
6. R. Zhu, H. Chen, T. Kosa, P. Coutino, G. Tan, and S. T. Wu, "High-ambient-contrast augmented reality with a tunable transmittance liquid crystal film and a functional reflective polarizer," J. Soc. Inf. Disp. **24**(4), 229–233 (2016).
7. F. Peng, F. Gou, H. Chen, Y. Huang, and S. T. Wu, "A submillisecond-response liquid crystal for color sequential projection displays," J. Soc. Inf. Disp. **24**(4), 241–245 (2016).
8. F. C. Lin, Y. P. Huang, C. M. Wei, and H. P. D. Shieh, "Color-breakup suppression and low-power consumption by using the Stencil-FSC method in field-sequential LCDs," J. Soc. Inf. Disp. **17**(3), 221–228 (2009).
9. S. T. Wu, "Nematic liquid crystal modulator with response time less than 100 μs at room temperature," Appl. Phys. Lett. **57**(10), 986–988 (1990).
10. T. D. Wilkinson, "Ferroelectric liquid crystal over silicon devices," Liquid Crystal Today **21**(2), 34–41 (2012).
11. A. Srivastava, V. Chigrinov, and H. S. Kwok, "Ferroelectric liquid crystals: Excellent tool for modern displays and photonics," J. Soc. Inf. Disp. **23**(6), 253–272 (2015).
12. L. Rao, S. He, and S. T. Wu, "Blue-phase liquid crystals for reflective projection displays," J. Disp. Technol. **8**(10), 555–557 (2012).
13. R. M. Hyman, A. Lorenz, S. M. Morris, and T. D. Wilkinson, "Polarization-independent phase modulation using a blue-phase liquid crystal over silicon device," Appl. Opt. **53**(29), 6925–6929 (2014).
14. Y. Chen, F. Peng, T. Yamaguchi, X. Song, and S. T. Wu, "High performance negative dielectric anisotropy liquid crystals for display applications," Crystals **3**(3), 483–503 (2013).
15. C. H. Wen, S. Gauza, and S. T. Wu, "High-contrast vertical alignment of lateral difluoro-terphenyl liquid crystals," Appl. Phys. Lett. **87**(19), 191909 (2005).
16. M. S. Brennesholtz, "New-technology light sources for projection displays," SID Int. Symp. Digest Tech. Papers **39**(1), 858–861 (2008).
17. K. Beeson, S. Zimmerman, W. Livesay, R. Ross, C. Livesay, and K. Livesay, "LED-based light-recycling light sources for projection displays," SID Int. Symp. Digest Tech. Papers **37**(1), 1823–1826 (2006).
18. H. Mönch, G. Derra, and E. Fischer, "Optimised light sources for projection displays," SID Int. Symp. Digest Tech. Papers **30**(1), 1076–1079 (1999).
19. M. Schadt, "Liquid crystal materials and liquid crystal displays," Annu. Rev. Mater. Sci. **27**(1), 305–379 (1997).

20. Y. Chen, F. Peng, and S. T. Wu, "Submillisecond-response vertically-aligned liquid crystal for color-sequential projection displays," J. Disp. Technol. **9**(2), 78–81 (2013).
21. S. T. Wu, U. Efron, and L. D. Hess, "Birefringence measurements of liquid crystals," Appl. Opt. **23**(21), 3911–3915 (1984).
22. I. Haller, "Thermodynamic and static properties of liquid crystals," Prog. Solid State Chem. **10**(2), 103–118 (1975).
23. S. T. Wu, "Birefringence dispersions of liquid crystals," Phys. Rev. A Gen. Phys. **33**(2), 1270–1274 (1986).
24. S. T. Wu and C. S. Wu, "Rotational viscosity of nematic liquid crystals A critical examination of existing models," Liq. Cryst. **8**(2), 171–182 (1990).
25. H. Chen, F. Peng, Z. Luo, D. Xu, S. T. Wu, M. C. Li, S. L. Lee, and W. C. Tsai, "High performance liquid crystal displays with a low dielectric constant material," Opt. Mater. Express **4**(11), 2262–2273 (2014).
26. H. Chen, M. Hu, F. Peng, J. Li, Z. An, and S. T. Wu, "Ultra-low viscosity liquid crystals," Opt. Mater. Express **5**(3), 655–660 (2015).

1. Introduction

Liquid-crystal-on-silicon (LCoS) display has found new applications in augmented reality (AR) such as Google Glass and Microsoft HoloLens, and vehicular head-up displays because of its high resolution density, low power consumption, lightweight and low cost [1–5]. In a wearable AR device, the displayed images are superimposed with the see-through real world. Thus, if the ambient light is bright, then the contrast ratio would be reduced dramatically. To enhance ambient contrast ratio, two approaches can be considered: (1) to use a smart dimmer to dynamically tune the intensity of incident ambient light [6], and (2) to boost the brightness of the LCoS display. To achieve high brightness, an effective approach is to use field sequential color (FSC) with red, green and blue LEDs [7]. By removing the spatial color filters, both optical efficiency and resolution density are improved significantly. Although FSC offers tremendous advantages, it demands liquid crystal (LC) response time to be faster than 1 ms in order to suppress color breakup [7, 8]. Therefore, the burden to achieve sub-millisecond response time falls on the employed LC material. On the device side, there are two additional constraints for a high-resolution LCoS backplane: (1) its maximum voltage is 6 V, limited by the wafer foundry's process, and (2) the commonly used overdrive and undershoot driving circuitry for improving LC response time [9] is usually not implemented because it could affect the accuracy of the pixel voltage. These constraints exert extra difficulties for the LC to achieve sub-millisecond response time.

To achieve sub-millisecond response time, several approaches have been investigated, including ferroelectric LCs [10, 101] and blue-phase LCs [12, 13]. Each technology has its own merits and demerits. For example, ferroelectric LC offers 100-μs response time, but it is bistable. Thus to obtain gray levels, we have to apply pulse width modulation, which dramatically increases the driving frequency and power consumption. On the other hand, blue phase requires a relatively high voltage, which is beyond what an LCoS device can afford.
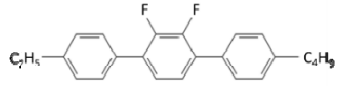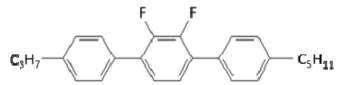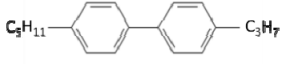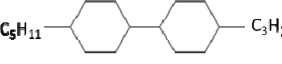
To overcome the abovementioned technical barriers, in this paper, we formulate a new nematic LC mixture, designated as UCF-N5, for LCoS display to achieve fast response time without the need of overdrive circuitry. UCF-N5 exhibits a relatively high birefringence (Δn = 0.15), ultra-low viscosity, and moderate negative dielectric anisotropy ($\Delta \varepsilon = -2.80$ @ 35°C). Its on-state voltage (V_{on}) is below 6 V. Meanwhile, high Δn enables the use of thin cell gap (d = 1.2 μm) to obtain high reflectance and sub-millisecond gray-to-gray (GTG) response time. Such a cell gap is still manageable for high-yield manufacturing. UCF-N5 is expected to find widespread applications for the emerging AR displays.

2. LC mixture formulation

Table 1 lists the compositions of UCF-N5. The base host is ZOC-7003 (JNC, Japan) [14]. It is a commercial mixture with Δn = 0.103 @ 550 nm, $\Delta \varepsilon = -4.36$, visco-elastic constant γ_1/K_{33} = 5.60 ms/μm^2, and clearing temperature T_c = 79°C. Its $\Delta \varepsilon$ is reasonably large, but the Δn and γ_1/K_{33} require further improvement. To boost Δn, we added two lateral difluoro-terphenyl

homologs (#2 & #3) [15], while to reduce viscosity we added ~25% non-polar diluters (#4 & #5).

Table 1. Chemical structures and compositions of UCF-N5.

No.	Compound Structure	Percentage (wt%)
1	ZOC-7003 (VA host)	43.0%
2	C_7H_5 —⟨⟩— (F F) —⟨⟩— C_4H_9	11.2%
3	C_3H_7 —⟨⟩— (F F) —⟨⟩— C_5H_{11}	20.8%
4	C_5H_{11} —⟨⟩—⟨⟩— C_3H_7	9.8%
5	C_5H_{11} —⟨⟩—⟨⟩— C_3H_7	15.2%

3. Material characterization

In experiment, we measured the dielectric anisotropy, birefringence, visco-elastic constant, and activation energy of UCF-N5. The obtained results are summarized in Table 2. For an LCoS projector using a high-brightness LED lamp, the panel temperature is about 35°C due to thermal effect [16, 17]. Therefore, all the data listed here are intended for 35°C operation. On the other hand, for an LCoS data projector using a high power arc lamp, the chassis temperature would be about 50°C~55°C [16, 18]. Here, we focus on the LCoS display using an LED lamp for wearable AR displays.

Table 2. Measured physical properties of UCF-N5 at T = 35°C, and f = 1 kHz.

	Δn @ λ=550 nm	$\varepsilon_{//}$	$\varepsilon_\perp$	$\Delta\varepsilon$	γ_1 (mPas)	K_{33} (pN)	γ_1/K_{33} (ms/µm²)	T_c (°C)	E_a (meV)
UCF-N5	0.1537	3.55	6.35	-2.80	53.4	13.9	3.83	77.1	264.0

3.1 Dielectric anisotropy

Dielectric anisotropy affects the operation voltage because V_{on} is proportional to $\sqrt{K_{33}/\Delta\varepsilon}$.

For a high resolution LCoS display, its maximum voltage is limited to 6 V. To lower the operation voltage, a large $\Delta\varepsilon$ helps, but the lateral polar groups dramatically increase the viscosity [19]. Thus, there exist contradicting requirements on $\Delta\varepsilon$ between low operation voltage and fast response time. A compromised $\Delta\varepsilon$ value is around −3. As a matter of fact, our UCF-N5 has $\Delta\varepsilon$ = −2.80 at 35°C. Later, we will prove that this $\Delta\varepsilon$ value is adequate to meet our voltage requirement, which is V_{on} < 6 V. The compositions in Table 1 represent a delicate balance between low operation voltage, manufacturable cell gap, and fast response time.

3.2 Temperature dependent birefringence

The cell gap of an LCoS panel can be made much thinner than that of a conventional large screen LCD panel (d ~3 µm). The main reason is LCoS device employs reflective mode, so

that its optical path is doubled. In theory, the required cell gap is 2x thinner than its transmissive counterpart with the same LC mixture. Small cell gap leads to faster response time (τ), as it is proportional to d^2. Using a high Δn LC mixture is another effective approach to lower the cell gap, which will further accelerate LC's relaxation process. For example, Chen et al. developed a VA mixture with $\Delta n = 0.191$ (at 550 nm and 50°C) for an LCoS panel with $d = 0.93$ µm [20]. It enables submillisecond response time, but such a thin cell gap is quite challenging for practical fabrications. To release this burden, we choose the cell gap of 1.2 µm, which is compatible to the current LCoS fabrication facility. Under such condition, the required Δn is 0.15 in order to obtain 100% normalized reflectance, i.e. $d\Delta n \sim$180 nm. By adjusting the weight percentage of each component in Table 1, our UCF-N5 shows $\Delta n = 0.154$ at $\lambda = 550$ nm and $T = 35$°C.
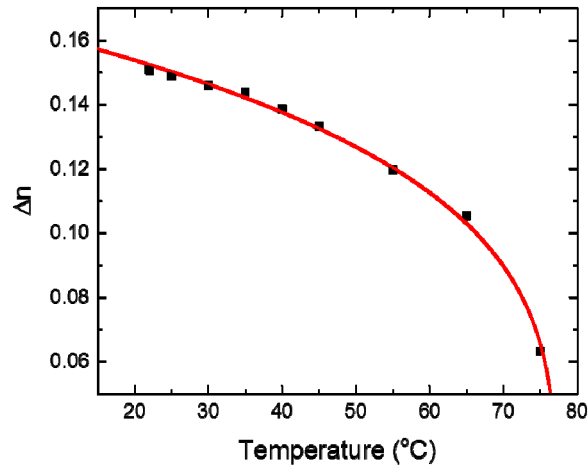

Fig. 1. Temperature dependent birefringence of UCF-N5 at $\lambda = 633$ nm. Dots are experimental data and solid line is fitting curve with Eq. (1).

Next, we measured the temperature dependent birefringence of UCF-N5 because our intended operating temperature is 35°C. In experiment, we filled UCF-N5 into a commercial VA cell with $d = 9.3$ µm. Then it was placed on a Linkam heating stage controlled by the temperature program (Linkam TMS94). Birefringence at each temperature was measured through phase retardation of the VA cell sandwiched between two crossed polarizers [21]. A He-Ne laser ($\lambda = 633$ nm) was used as the probe beam. The obtained results are plotted in Fig. 1, where black dots represent the measured data and red solid line is the fitting curve using Haller's semi-empirical equation [22]:

$$\Delta n(T) = \Delta n_0 S = \Delta n_0 (1 - T / T_c)^\beta, \tag{1}$$

where Δn_0 is the extrapolated birefringence at $T = 0$, S is the order parameter, and β is a material constant. Through fitting, we found $\Delta n_0 = 0.246$ and $\beta = 0.259$ for UCF-N5.

3.3 Wavelength dependent birefringence

To investigate the electro-optical performances at the specified RGB colors, we measured the birefringence dispersion at 35°C. During the measurement, a tunable Argon ion laser (457 nm, 488 nm and 514 nm) and a He-Ne laser were used as probe beams. Figure 2 shows the obtained results, in which black dots represent the measured data and red solid line is the fitting curve using single-band birefringence dispersion equation [23]:

$$\Delta n = G \frac{\lambda^2 \lambda^{*2}}{\lambda^2 - \lambda^{*2}}, \tag{2}$$

where G is a proportionality constant and λ^* is the mean resonance wavelength. Through fitting, we found $G = 1.8936$ μm^{-2} and $\lambda^* = 0.2574$ μm. From Eq. (2), we can calculate the birefringence at the RGB wavelengths we want. Results (at 35°C) are $\Delta n = 0.1780$ at $\lambda = 450$ nm, 0.1537 at 550 nm, and 0.1423 at 650 nm. These data will be used later for calculating the voltage-dependent reflectance.
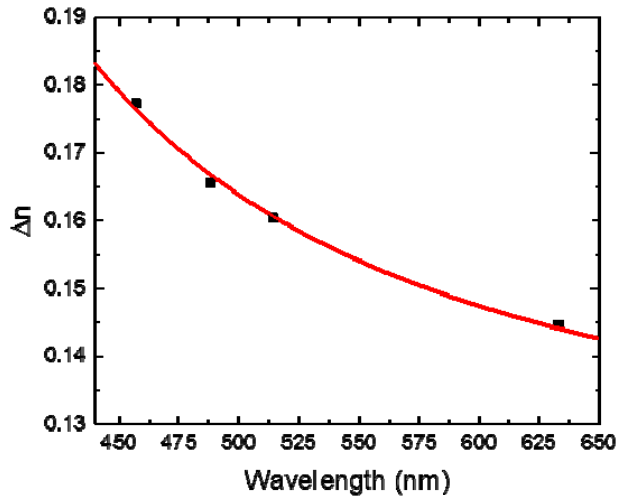

Fig. 2. Wavelength dependent birefringence of UCF-N5 at $T = 35$°C. Dots are experimental data and solid line is fitting curve with Eq. (2).

3.4 Temperature dependent visco-elastic constant

By measuring the time-dependent relaxation process of a VA cell, we can extract the visco-elastic constant (γ_1/K_{33}). The LC response time is linearly proportional to γ_1/K_{33}, which is highly dependent on the temperature, as described by the following equation [24]:

$$\frac{\gamma_1}{K_{33}} = \frac{a \cdot \exp(E_a / k_B T)}{(1 - T / T_c)^\beta},$$　　　(3)

where a is a proportionality constant, E_a is the activation energy and k_B is the Boltzmann constant. From Eq. (3), γ_1/K_{33} increases exponentially as the temperature decreases. This explains why LCoS response time at 35°C (with an LED lamp) is much slower that that at 50°C (with a high power arc lamp). In Eq. (3), activation energy (E_a) plays the key role; it determines the rising rate of γ_1/K_{33} [25, 26].

In experiment, we measured γ_1/K_{33} at different temperatures, and fitted the measured data. Results are plotted in Fig. 3. The obtained activation energy is 264.0 meV. At 35°C, its γ_1/K_{33} is only 3.83 ms/μm^2, which originates from high concentration of diluters. The corresponding rotational viscosity (γ_1) is 53.4 mPas and bend elastic constant (K_{33}) is 13.9 pN.
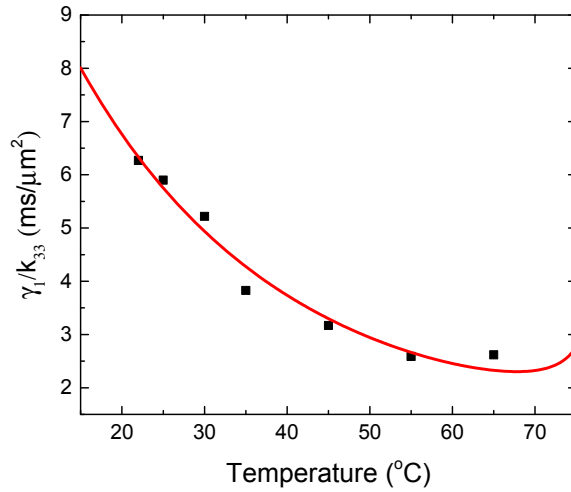
Fig. 3. Temperature dependent γ_1/K_{33} of UCF-N5. Dots are experimental data and solid line is fitting curve with Eq. (3).

4. Simulation results

The electro-optical performance of UCF-N5 in a VA LCoS device is characterized using a commercial LCD simulator DIMOS 2.0. In simulation, we set the cell gap at 1.2 μm, to be compatible with current fabrication capability. We used the material parameters (at 35°C) listed in Table 2. As for VA LCoS, the pretilt angle is controlled at 88°, and the azimuthal angle is 45° w.r.t. the optic axis of the polarizing beam splitter (PBS). An aluminum reflector is placed on the inner surface of the VA cell. Figure 4 shows the simulated voltage-dependent reflectance (VR) curves for the RGB primary colors. For green light (550 nm), its peak voltage is 5.7 V, but if we are willing to sacrifice 2% reflectance (98.3%), we can get $V_{on} \approx 5$ V. Low power consumption is expected.
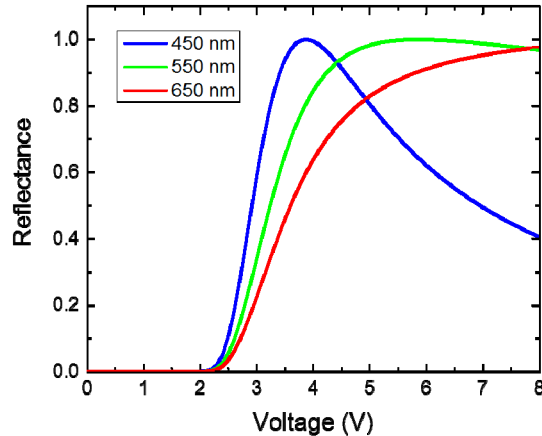

Fig. 4. Simulated VR curves of a VA LCoS using UCF-N5. Cell gap $d = 1.2$ μm.

To study the GTG response time of our VA LC device, we divided the VR curve (550 nm) into eight gray levels equally and calculated the response time between different gray levels. Table 3 lists the detailed reflectance and driving voltage of each corresponding gray level. As usual, the response time is defined as the time interval between 10% and 90% reflectance. Results are summarized in Table 4. During our calculations, no overdrive and undershoot voltage was applied. From Table 4, we find the rise time is 0.32 ms and decay time is 0.47 ms

between gray levels 1 and 8. The average GTG rise time is 0.86 ms and the decay time is 0.91 ms. With such a fast response time, image blur and color breakup can be greatly suppressed. As far as we know, this is the first demonstration for achieving sub-millisecond response time at 35°C without the assistance of overdrive and undershoot effects. Besides, it is realized using a practical cell gap ($d = 1.2$ µm).

Table 3. Reflectance and driving voltage for each corresponding gray level.

Gray level	1	2	3	4	5	6	7	8
Reflectance	0	14.0%	28.1%	42.1%	56.2%	70.2%	84.3%	98.3%
Voltage (V)	0	2.67	2.93	3.12	3.35	3.60	3.98	5.00

Table 4. Calculated (left) and measured (right) GTG response time of the reflective VA cell at $T = 35$°C. (unit: ms)

	1	2	3	4	5	6	7	8
1		2.92/2.75	2.07/1.95	1.58/1.48	1.25/1.29	0.97/0.97	0.69/0.69	0.32/0.37
2	0.36/0.35		1.65/1.36	1.26/1.34	1.05/1.10	0.85/0.91	0.60/0.65	0.28/0.33
3	0.36/0.35	1.26/1.14		1.14/1.06	0.97/1.00	0.78/0.77	0.56/0.62	0.25/0.31
4	0.37/0.36	1.49/1.47	1.29/0.93		0.93/0.78	0.76/0.72	0.54/0.52	0.25/0.30
5	0.38/0.40	1.38/1.39	1.22/1.01	1.07/0.79		0.74/0.56	0.52/0.48	0.23/0.28
6	0.41/0.42	1.31/1.36	1.19/1.05	1.03/0.94	0.89/0.69		0.52/0.46	0.23/0.27
7	0.43/0.45	1.27/1.34	1.16/1.21	1.03/0.98	0.72/0.75	0.74/0.57		0.23/0.23
8	0.47/0.50	1.27/1.33	1.16/1.24	1.05/1.04	0.92/0.90	0.78/0.74	0.61/0.51	

To validate the simulation results listed in Table 4, in experiment we prepared a VA test cell with cell gap $d = 2.4$ µm, and measured its response time at transmissive mode. In a reflective LCoS device, its cell gap is 2x thinner than that of our test cell. As a result, the response time should be 4x faster than the measured one. Taking this factor into consideration, we obtained the GTG response time at 35°C experimentally. Results are also included (at the right side) in Table 4. Overall speaking, the agreement with simulation results is reasonably good. We find that the measured average GTG rise time is 0.84 ms and decay time is 0.86 ms. We believe UCF-N5 would find widespread applications for the emerging wearable displays, vehicle displays, as well as pico-projectors.

5. Conclusion

We have developed a new LC mixture UCF-N5 with an ultra-low viscosity ($\gamma_1 = 53.4$ mPas @ 35°C) and moderate dielectric anisotropy ($\Delta\varepsilon = -2.80$ @ 35°C). When employed into a VA LCoS projector with a LED lamp, we can achieve sub-millisecond response time without the complicated overdrive circuitry. Moreover, the operation voltage is below 6 V. With such a fast response time, image blur and color breakup can be greatly suppressed. Moreover, its 1.2-µm cell gap is relatively easy to fabricate in mass production. Potential application of UCF-N5 for the emerging wearable AR displays is foreseeable.